Journal of Statistical Physics, Vol. 75, Nos. 5/6, 1994

Validation of a Monte Carlo Simulation of the Plane Couette Flow of a Rarefied Gas

Carlo Cercignani[1] and Stefano Cortese[1]

Received January 21, 1994

We report and discuss the results of a direct Monte Carlo simulation of the flow of a rarefied gas flowing between two parallel plates when one of them moves in its own plane. The boundary conditions are assumed to be of the "bounce-back" type and the molecules to be Maxwell's. Under this condition the moments can be computed exactly, following a method used by Ikenberry and Truesdell in the unbounded case. This allows a comparison of the Monte Carlo methods with the exact solution and an evaluation of its accuracy.

KEY WORDS: Kinetic theory; direct simulation; Couette flow.

1. INTRODUCTION

While the Monte Carlo techniques for solving the Boltzmann equation[1-3] have been used for some time now, the problem of their validation in the space-inhomogeneous case through a comparison with an exact solution does not appear to have been treated so far. This circumstance is clearly related to the difficulty of finding exact solutions for the inhomogeneous Boltzmann equation in general, and for the inhomogeneous case in the presence of boundaries in particular.[4] It is clear, however, that the study of this problem is of great importance for understanding the accuracy and the range of applicability of the Monte Carlo method. Here we point out that, using the "bounceback"[5] boundary conditions, it is possible to find exact expressions for a few moments of the distribution function in the plane Couette flow problem, when the molecules are assumed to be Maxwell's. Actually this closed-form expression had already been found by Ikenberry and Truesdell,[6] who did not mention any boundaries. This is

[1] Dipartimento di Matematica, Politecnico di Milano, Milan, Italy. CARCER @ipmmal.polimi.it.

0022-4715/94/0600-0817$07.00/0

possible because, as remarked before by Cercignani,[5] there is no Knudsen layer at the boundaries for the solution under consideration and hence the solution can be continued to the entire space.

In this paper we shall discuss the aforementioned closed-form solution, the Monte Carlo solution, and the fluctuations of the macroscopic quantities. The simulations have been performed with both a one-dimensional and a two-dimensional code and found in a good agreement with the closed-form solution. Our results refer to Knudsen numbers Kn of order 10^{-1} and Mach numbers Ma from 0.5 to 31. The solution has, however, such similarity properties that only the combination $\mathrm{Kn} \cdot \mathrm{Ma}$ is significant. The latter product ranges from 0.1 to 6.2.

2. BASIC EQUATIONS

Let us consider a monatomic rarefied gas with average density ρ_0 in motion between two parallel plates, located at $y=0$ and $y=L$, respectively (see Fig. 1). The upper plate moves with velocity U_0, while the lower one is at rest. The Boltzmann equation reads as follows[2,3,7]:

$$\frac{\partial f}{\partial t}+\xi_1\frac{\partial f}{\partial x}+\xi_2\frac{\partial f}{\partial y}+\xi_3\frac{\partial f}{\partial z}=Q(f,f) \tag{2.1}$$

where $\mathbf{x}=(x, y, z)$ and $\xi=(\xi_1, \xi_2, \xi_3)$ are the position and velocity vectors, respectively, of a molecule while

$$Q(f,f)=\frac{1}{m}\iint (f'f'_*-ff_*)\,B(\theta, |\xi-\xi_*|)\,d\xi_*\,d\theta\,d\varepsilon \tag{2.2}$$

is the collision operator. Here $B(\theta, |\xi-\xi_*|)$ is a kernel describing the details of molecular interaction, m is the molecular mass, and f', f'_*, and f_* are the same as f, except for the fact that ξ is replaced by ξ', ξ'_*, and

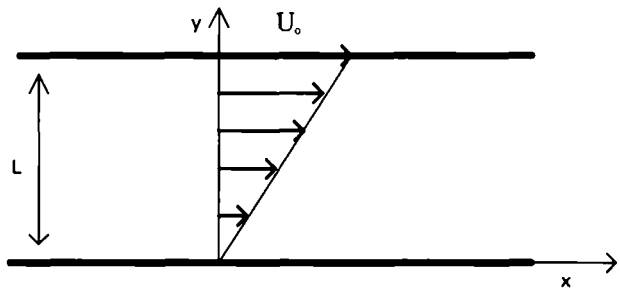

Fig. 1. Geometry and velocity profile.

ξ_*, respectively. Also, ξ_* is an integration variable (the velocity of any molecule colliding with a molecule of velocity ξ), whereas ξ' and ξ'_* are the velocities of two molecules entering a collision which brings them to velocities ξ and ξ_*. Finally, θ and ε give the direction along which the same molecules approach each other.

The dimensionless parameters here are the Knudsen number Kn_L based on the distance between the plates L ($\mathrm{Kn}_L = \lambda_0/L$), and the speed ratio $S = U_0/V_{\mathrm{th}}$ [where $V_{\mathrm{th}} = (2RT_0)^{1/2}$ is the thermal speed], related to the Mach number Ma by $\mathrm{Ma} = (6/5)^{1/2} S = 1.095S$. The basic parameter should be the product of these two parameters, or the dimensionless velocity gradient

$$\kappa = \frac{U_0 \lambda_0}{L(RT_0)^{1/2}} \tag{2.3}$$

We complete our formulation with the following initial and boundary conditions:

(a) At time zero we assume a Mawellian distribution with temperature T_0 and bulk velocity $U_0\, y/L$ along the x axis:

$$f(0, x, y, \xi) = \rho_0 \pi^{-3/2} V_{\mathrm{th}}^{-3} \exp(-|\xi_1 - \mathbf{i} U_0\, y/L|^2 / V_{\mathrm{th}}^2) \tag{2.4}$$

where $\mathbf{i}$ is the unit vector along the x axis.

(b) At the plates we assume that the molecules bounce back in the reference frame of each plate and hence write

$$f(t, x, 0, \xi) = f(t, x, 0, -\xi) \tag{2.5}$$

$$f(t, x, L, \xi) = f(t, x, L, 2U_0 - \xi) \tag{2.6}$$

In the two-dimensional simulation a periodicity condition (with period $\hat{L}$) was added in the x direction. If we assume Maxwell's molecules,[2,3] we have

$$B(\theta, |\xi - \xi_*|) = B(\theta) \tag{2.7}$$

Then the mean free time will be independent of temperature and thus constant if the density keeps constant. As a matter of fact, the model used in our calculations is the variable hard-sphere model (VHS); this means that if the collision law between particles is the same as for hard spheres [and hence $B(\theta, |\xi - \xi_*|) = \sigma^2 |\xi - \xi_*| \cos\theta \sin\theta$, where σ is the sphere diameter], we allow this diameter to be inversely proportional to the power $2/(\eta - 1)$ of the relative speed (here η is the exponent of the repelling

force in the corresponding inverse power law model). Thus, to mimic Maxwellian molecules, we take $\sigma = \sigma_0 (V_0/V)^{1/2}$, where $V = |\xi - \xi_*|$ is the relative speed and V_0 its average value at the reference temperature. Thus Eq. (2.7) remains true.

3. THE CLOSED-FORM SOLUTION

One can obtain a space-inhomogeneous solution for the Boltzmann equation from a homogeneous one by means of Nikol'skii's transformation.[8,6,7] Thus, by applying this transformation to the BKW mode, one obtains a solution first obtained by Muncaster.[9] Nikol'skii's solutions describe a spherical expansion or a spherical compression; the latter ceases to exist for a finite time. Their moments are space-homogeneous; this applies in particular to the thermal energy per unit volume of the gas. Solutions of this kind for the moments were first found by Galkin and are called homoenergetic dilatations.[10,7]

Homoenergetic dilatations are particular cases of more general solutions called homoenergetic affine flows. The book by Truesdell and Muncaster[7] gives a unified discussion of homoenergetic affine flows. The defining properties are the following:

(a) The body force (per unit mass) $\mathbf{X}$ acting on the molecules is constant:

$$\mathbf{X} = \text{const} \tag{3.1}$$

(b) The moments formed with the peculiar velocity $\mathbf{c} = \xi - u_0$ are space-homogeneous.

(c) The bulk velocity $\mathbf{u}$ is an affine function of position $\mathbf{x}$:

$$\mathbf{u} = \mathbf{K}(t)\,\mathbf{x} + \mathbf{u}_0(t) \tag{3.2}$$

An analysis of the balance equations based on (a)–(c) immediately leads to the following restrictions on $\mathbf{K}$ and $\mathbf{u}_0$:

$$\begin{cases} \dot{\mathbf{K}} + \mathbf{K}^2 = 0 \\ \dot{\mathbf{K}}\mathbf{v}_0 + \mathbf{K}\mathbf{u}_0 = \mathbf{X} \end{cases} \tag{3.3}$$

The general solution of this system is

$$\begin{cases} \mathbf{K}(t) = [\mathbf{I} + t\mathbf{K}(0)]^{-1}\,\mathbf{K}(0) \\ \mathbf{u}_0(t) = [\mathbf{I} + t\mathbf{K}(0)]^{-1}\,[\mathbf{u}_0(0) + t\mathbf{X} + \tfrac{1}{2}t\mathbf{K}(0)\,\mathbf{X}] \end{cases} \tag{3.4}$$

where $\mathbf{I}$ is the 3×3 identity matrix. This solution exists globally for $t > 0$ if the eigenvalues of $\mathbf{K}(0)$ are nonnegative; otherwise the solution ceases to exist for $t = t_0$, where $-t_0^{-1}$ is the largest, in absolute value, among the negative eigenvalues of $\mathbf{K}(0)$.

In particular, if

$$[\mathbf{K}(0)]^2 = 0 \tag{3.5}$$

then $[\mathbf{I} + t\mathbf{K}(0)]^{-1} = \mathbf{I} - t\mathbf{K}(0)$ and therefore $\mathbf{K}(t)$ is independent of time. $\mathbf{u}$ is then steady if and only if

$$\mathbf{K}(0)\,\mathbf{X} = \mathbf{0} \tag{3.6}$$

and if $\mathbf{u}_0(0)$ is chosen in such a way that

$$\mathbf{K}(0)\,\mathbf{u}_0(0) = \mathbf{X} \tag{3.7}$$

In particular, this is always possible if $\mathbf{X} = \mathbf{0}$.

Equation (3.5) is satisfied if and only if a coordinate system exists for which the matrix representation of $\mathbf{K}(0)$ is given by

$$((K_{ij})) = \begin{pmatrix} 0 & K & 0 \\ 0 & 0 & 0 \\ 0 & 0 & 0 \end{pmatrix} \tag{3.8}$$

For a simple proof of this, see ref. 11. When (3.5) applies, one talks, for obvious reasons, of a homoenergetic shear flow.

As shown by Galkin[10,12–14] and Truesdell,[15] the second-order moment equations for a Maxwell gas, associated with a homoenergetic affine flow, are decoupled from those of higher order and can be solved explicitly. This result generalizes the result mentioned above for homoenergetic dilatations.

The most interesting moment equations are those for $p_{yy} = \int c_y^2 f\, d\xi$, $p_{xy} = \int c_x c_y f\, d\xi$, and $p = \frac{1}{3}\int |\mathbf{c}|^2 f\, d\xi$:

$$\begin{aligned} \tau\dot{p} + \tfrac{2}{3}\mathscr{T} p_{xy} &= 0 \\ \tau\dot{p}_{xy} + p_{xy} + \mathscr{T} p_{yy} &= 0 \\ \tau\dot{p}_{yy} - p + p_{yy} &= 0 \end{aligned} \tag{3.9}$$

Here τ is the relaxation time, given by

$$\tau = \mu/p \tag{3.10}$$

where μ is the viscosity of the gas when the Boltzmann equation agrees with the Navier–Stokes equations, while $\mathscr{T}$ is the dimensionless number

$$\mathscr{T} = \tau K = \frac{\mu}{p} K \tag{3.11}$$

This is a system of three linear, homogeneous, first-order differential equations that possesses a set of linearly independent solutions of the form

$$p = p^0 \exp(\chi t/\tau); \qquad p_{xy} = p^0_{xy} \exp(\chi t/\tau); \qquad p_{yy} = p^0_{yy} \exp(\chi t/\tau) \tag{3.12}$$

where χ is one of the roots of the third-degree equation

$$\chi(\chi + 1)^2 = \tfrac{2}{3}\mathscr{T}^2 \tag{3.13}$$

This equation can be solved explicitly by means of the formulas of Scipione del Ferro and Cardano. It is enough here to remark that it certainly has a real root R; the other two roots can be easily expressed in terms of R and turn out to be complex with real part $-1 - R/2$ and imaginary part $\pm[R(1 + 3R/4)]^{1/2}$. This immediately shows that R must be positive, because the product of the roots must equal the right-hand side of Eq. (3.13). Thus, in general, the solution of system (3.9) will possess a part that grows exponentially in time and another part that oscillates with an exponentially decaying amplitude. The asymptotically dominating part agrees with the Navier–Stokes equations with an error $O(\mathscr{T}^2)$. The exponential growth of the dominating part can be easily explained by the circumstance that the solution under consideration forbids any heat diffusion; thus the work done by the tangential stress heats up the gas and increases the pressure, which in turn increases the stress components p_{yy} and p_{xy} because viscosity increases with pressure.

Condition (b) above holds for the solutions obtained by Truesdell[15] and Galkin.[10,12–14] For analyses relating directly to the distribution function f, this condition is transformed[11] into:

(b′) The variable $\mathbf{x}$ appears in f only through the bulk velocity

$$f = f(\mathbf{c}, t) \tag{3.14}$$

where $\mathbf{c} = \boldsymbol{\xi} - \mathbf{u}$ is the random velocity. In ref. 11, Cercignani attacked the problem of showing that the conditions given above are also sufficient for a solution of the Boltzmann equation for homoenergetic affine flows to exist. In particular he showed that $f(\mathbf{c}, t)$ must satisfy the equation

$$\frac{\partial f}{\partial t} - \frac{\partial f}{\partial \mathbf{c}} \cdot \mathbf{K}\mathbf{c} = Q(f, f) \tag{3.15}$$

and proved an existence theorem for Eq. (3.15), not only for Maxwell's molecules, but for general kernels, as explained by the following.

Existence Theorem. There exists a solution f of Eq. (1.1), where the kernel $B(\xi - \xi_*, \mathbf{n})$ of the collision term $Q(f, f)$ does not grow more than quadratically in ξ and ξ_* and the initial mass density, energy density, and H-functional $(= \int f \log f \, d\xi)$ are finite at time 0. These functionals remain bounded for $0 \leqslant t \leqslant T$. The time T is arbitrary provided $\mathbf{K}(0)$ has no negative eigenvalues. If $\mathbf{K}(0)$ possesses negative eigenvalues and t_0^{-1} is their largest absolute value, then T must not be larger than t_0.

One can also prove[11] the following.

Uniqueness Theorem. Let f be the solution delivered by the Existence Theorem. If the fourth-order moments exist at $t = 0$, they exist in $[0, T]$, and then the solution of Eq. (3.10) is unique.

Although we have not mentioned boundary conditions so far in this section, it is now easy to check that solutions of the form $f = f(\mathbf{c}, t)$ satisfy the boundary conditions (2.5) and (2.6) provided the initial distribution is even in $\mathbf{c}$ and $\mathbf{u}(y = 0) = 0$ and $\mathbf{u}(y = L) = U_0\mathbf{i}$.

4. METHOD OF SOLUTION

The Monte Carlo simulation was devised in agreement with the formulation of Section 2. We considered both a one-dimensional and a two-dimensional simulation. In the present description of the method we consider the two-dimensional case; the modifications for the one-dimensional one are obvious.

The basic steps of the simulation are as follows:

(a) The time interval $[0, T]$ over which the solution was sought for was subdivided into subintervals with step Δt.

(b) The space domain was subdivided into cells with sides Δx, Δy.

(c) The gas molecules were simulated in the gap G with a stochastic system of N points having positions $x_i(t)$, $y_i(t)$ and velocities $\xi_i(t)$.

(d) At each time there are N_m molecules in the mth cell; this number is varied by computing its evolution in the following two stages:

Stage 1. The binary collisions in each cell are calculated without moving the particles.

Stage 2. The particles are moved, with the new initial velocities acquired after collision (no collisions in this stage).

(e) Stages 1 and 2 are repeated until $t = T$.

(f) The important moments of the distribution functions are calculated by averaging over the particle in a cell. An additional space averaging is introduced for moments which are space-homogeneous.

Let us describe now the two stages of the calculation in some detail:

Stage 1. We use Bird's "no time counter" scheme,[1] which envisages the following three steps:

Step 1. Computation of the maximum number of binary collisions in a box, N_{cmax}. This is, for our model, independent of the relative speed and thus it represents the average number of collisions that must occur in a time interval Δt.

Step 2. The effective number of collisions N_{coll} that occur in the current time interval is a Poisson statistical variable with mean N_{cmax} which is simulated by counting the number of random delays between successive collisions drawn from the corresponding exponential distribution until the time interval is expired.

Step 3. Choose N_{coll} pairs (i, j) of particles randomly. Each of these pairs is "collided" with probability $|\xi_i - \xi_j| / \langle |\xi_i - \xi_j| \rangle_{\max}$ raised to the power $(5-\eta)/(\eta-1)$ which becomes certainty for Maxwell molecules. If the collisional event occurs, the velocities after collisions are calculated in the following way:

$$\xi_i^+ = \tfrac{1}{2}(\xi_i + \xi_j + \mathbf{k}\,|\xi_i - \xi_j|) \tag{4.1}$$

$$\xi_j^+ = \tfrac{1}{2}(\xi_i + \xi_j - \mathbf{k}\,|\xi_i - \xi_j|) \tag{4.2}$$

where $\mathbf{k}$ is a vector randomly distributed on the unit sphere. Otherwise the velocities are left unchanged.

Stage 2. The new positions of the molecules are computed through the equations

$$\begin{aligned} x_i^+ &= x_i + \xi_{1i}\,\Delta t \\ y_i^+ &= y_i + \xi_{2i}\,\Delta t \end{aligned} \tag{4.3}$$

The particles with $y_i^+ \leqslant 0$ or $y_i^+ \geqslant L$ are reflected according to Eqs. (2.5)–(2.7); the particles with $x_i^+ \leqslant 0$ and $x_i^+ \geqslant \hat{L}$ are reinjected at $x_i^+ + \hat{L}$ or $x_i^+ - \hat{L}$ with their velocities.

Table I. Values of the Parameters Used in the Simulations

Knudsen number	Mach number	non-dimensional velocity gradient	time constant χ	sampling step (in units $\lambda_0/\sqrt{RT_0}$)
0.2	0.5	0.162	0.017	0.4
0.2	3	0.97	0.346	0.2
0.2	31	10.04	3.43	0.1

5. RESULTS OF THE ONE-DIMENSIONAL SIMULATION

In the one-dimensional simulation we used 100 cells with $N = 10{,}000$ particles per cell and collected data only at the end of certain chosen intervals of length $T \gg \Delta t$. As time unit we chose the mean free time and as length unit the mean free path. Then the data for our calculations are summarized in Table I.

The results for the moments p_{xy}, p_{yy}, their ratio, and the "longitudinal temperature" $T_x = p_{xx}/\rho R$ and the dimensionless velocity are given in Figs. 2–6 (for $\mathscr{T} = 0.162$ and $\Delta y = 0.05$), Figs. 7–11 (for $\mathscr{T} = 0.97$, $\Delta y = 0.05$), and Figs. 12–16 (for $\mathscr{T} = 10.04$, $\Delta y = 0.1$). The fields of T_x and U_x are snapshots taken at the final time and are plotted along the plate distance together with the linear interpolation and error bounds given by $\pm 3(T_x/N)^{1/2}$ for U_x and $\pm 3T_x(2/N)^{1/2}$ for T_x, while the time evolution of the stresses is averaged over all the cells thanks to the spatial homogeneity.

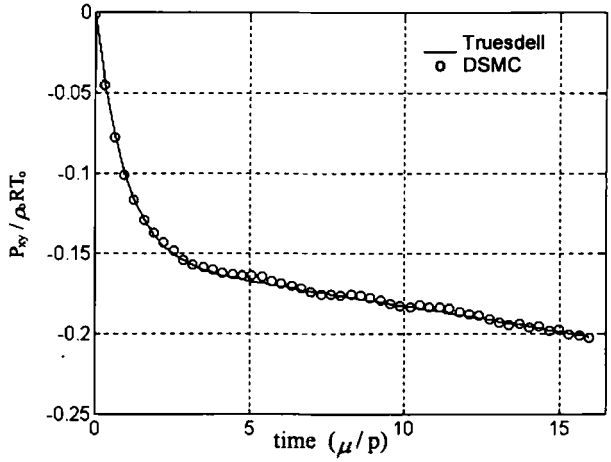

Fig. 2. Time evolution of tangential stress; Kn = 0.2, Ma = 0.5 (one-dimensional simulation).

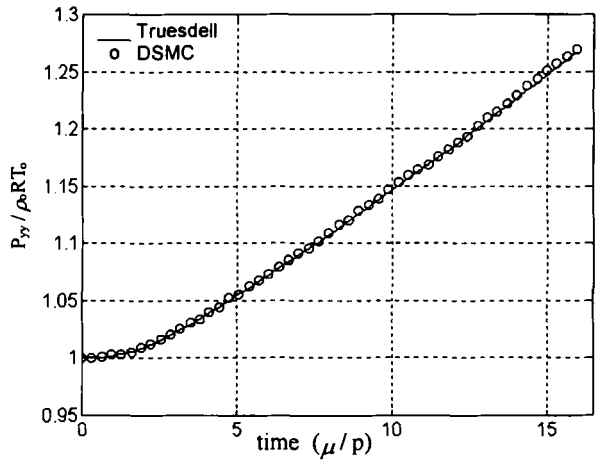

Fig. 3. Time evolution of the stress normal to the flow; Kn = 0.2, Ma = 0.5 (one-dimensional simulation).

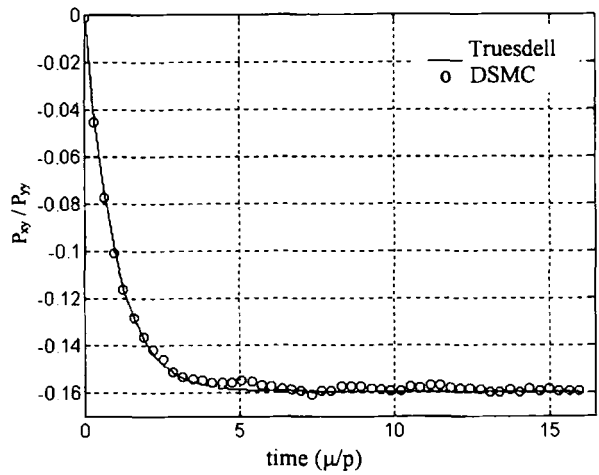

Fig. 4. Time evolution of the ratio of the tangential to the normal stress; Kn = 0.2, Ma = 0.5 (one-dimensional simulation).

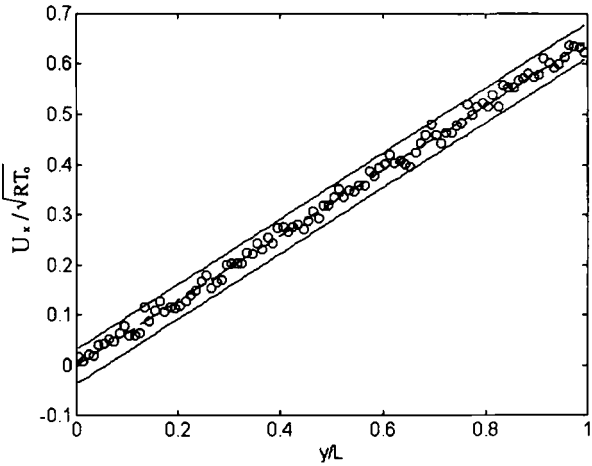

Fig. 5. Tangential velocity profile at the final instant; Kb = 0.2, Ma = 0.5: (○) one-dimensional DSMC, (--) linear fit, (—) ±3 standard deviations obtained through the calculated temperature T_x.

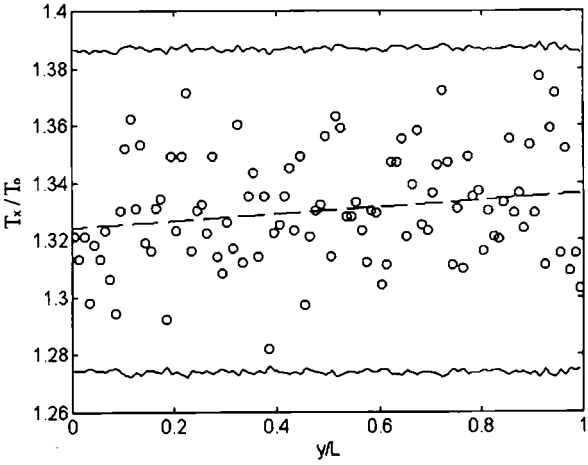

Fig. 6. T_x at the final instant; Kn = 0.2, Ma = 0.5: (○) one-dimensional DSMC, (--) linear fir, (—) ±3 standard deviations from the mean.

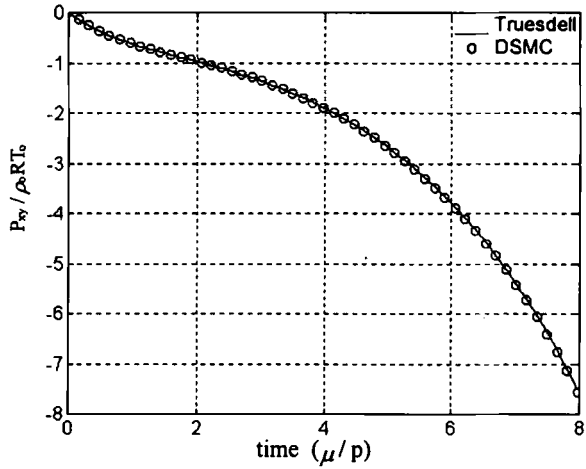

Fig. 7. Time evolution of tangential stress; Kn = 0.2, Ma = 3 (one-dimensional simulation).

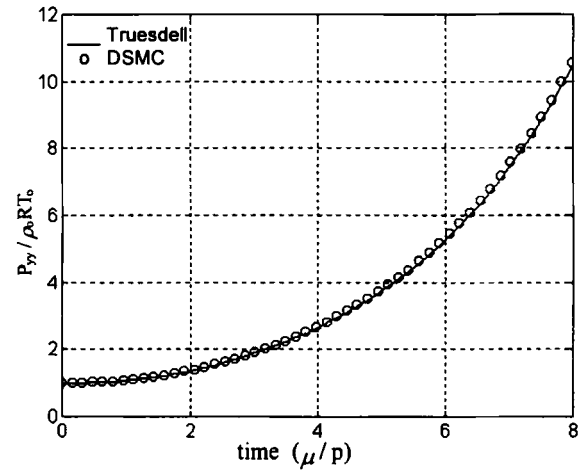

Fig. 8. Time evolution of the stress normal to the flow; Kn = 0.2, Ma = 3 (one-dimensional simulation).

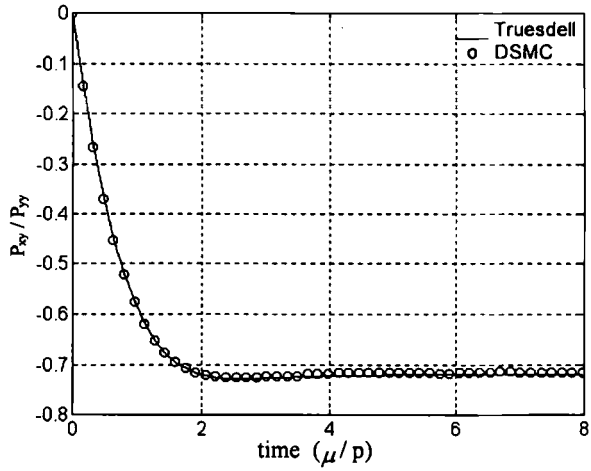

Fig. 9. Time evolution of the ratio of the tangential to the normal stress; Kn = 0.2, Ma = 3 (one-dimensional simulation).

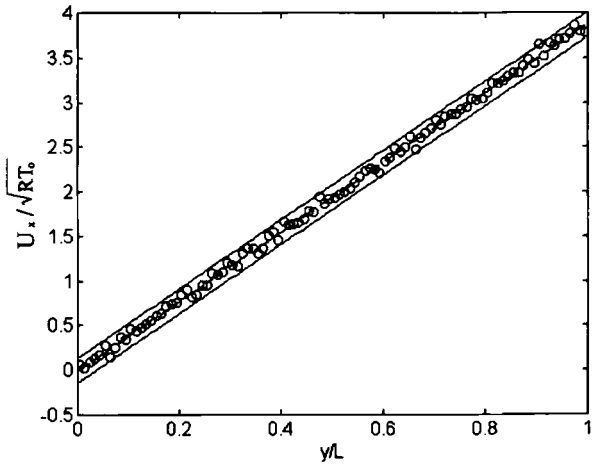

Fig. 10. Tangential velocity profile at the final instant; Kn = 0.2, Ma = 3: (○) one-dimensional DSMC, (--) linear fit, (—) ±3 standard deviations obtained through the calculated temperature T_x.

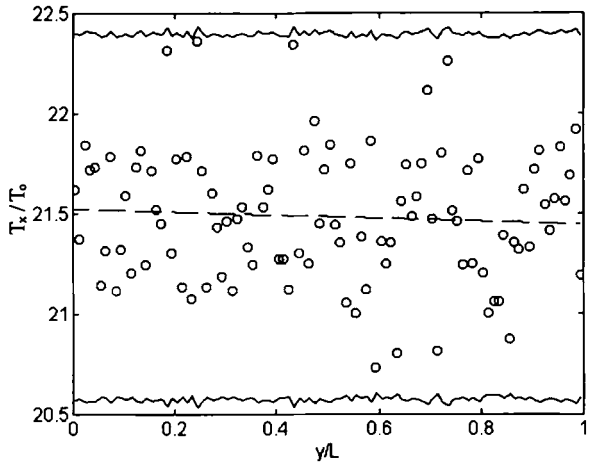

Fig. 11. T_x at the final instant; Kn = 0.2, Ma = 3: (○) one-dimensional DSMC, (--) linear fit, (—) ±3 standard deviations from the mean.

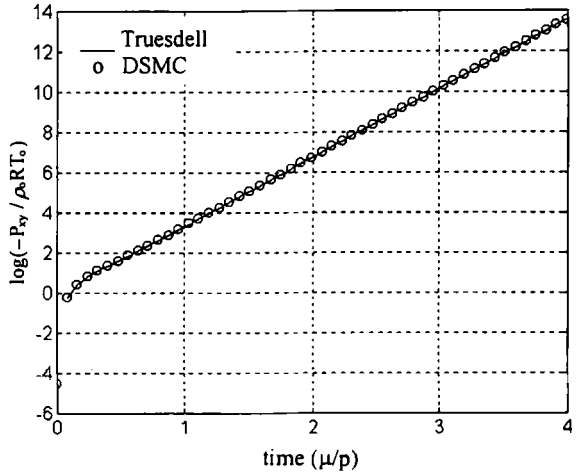

Fig. 12. Time evolution of tangential stress; Kn = 0.2, Ma = 31 (one-dimensional simulation).

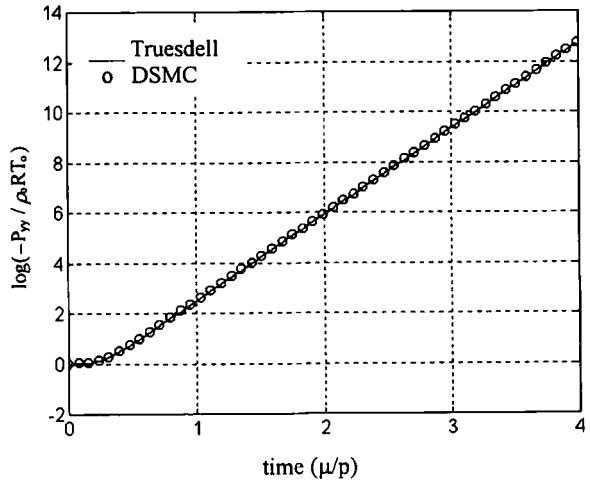

Fig. 13. Time evolution of the stress normal to the flow; Kn = 0.2, Ma = 31 (one-dimensional simulation).

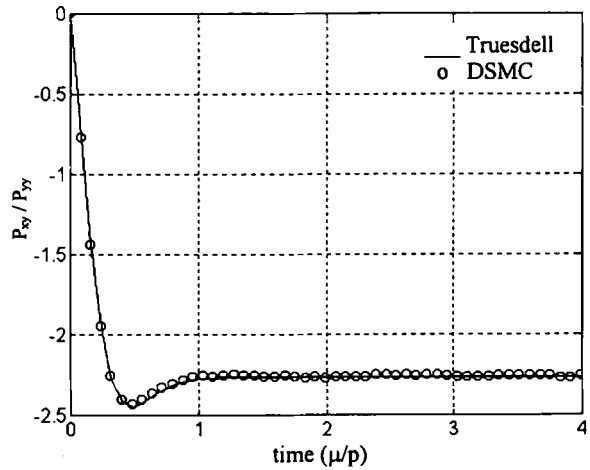

Fig. 14. Time evolution of the ratio of the tangential to the normal stress; Kn = 0.2, Ma = 31 (one-dimensional simulation).

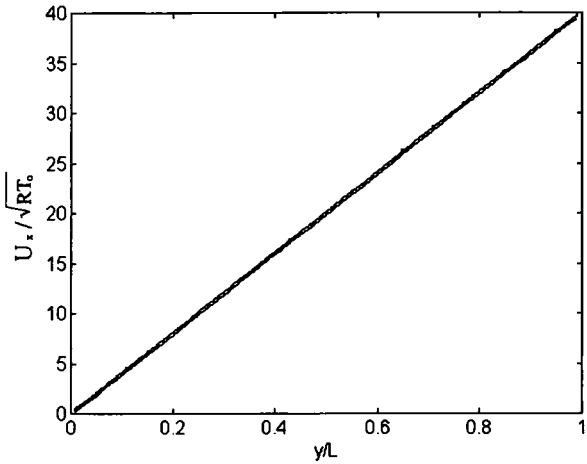

Fig. 15. Tangential velocity profile at $0.96\mu/p$; Kn = 0.2, Ma = 31: (·) one-dimensional DSMC with 50 cells and 40,000 particles per cell, (—) ±3 standard deviations obtained through the calculated temperature T_x.

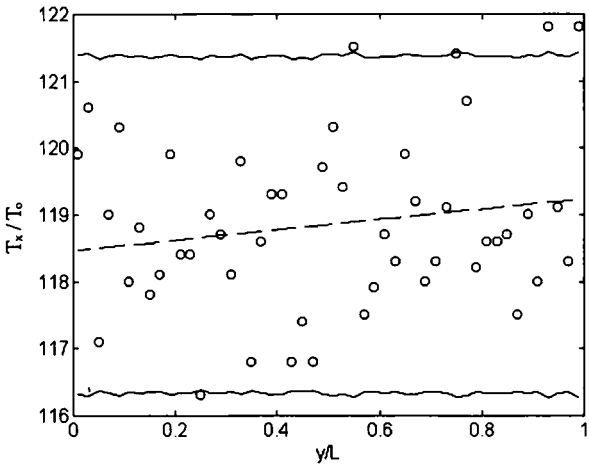

Fig. 16. T_x at $0.96\mu/p$; Kn = 0.2, Ma = 31: (○) one-dimensional DSMC, (--) linear fit, (—) ±3 standard deviations from the mean.

From these pictures it is easy to verify the following expectations, based on the discussion of Section 3.

(a) There is an unsteady solution with constant density, while the stresses are uniform and the velocity profile is steady. Remark that the latter is verified by linear interpolation at a given time instant.

(b) Interchanging the values of the Mach and Knudsen numbers has no consequences thanks to the dynamical self-similarity of the flow, which implies that the solution only depends on the product of these two numbers.

(c) The time evolution corresponds to the solution given by Truesdell and summarized in Section 3.

We remark that the fluctuations are large, but in the case of the bulk velocity they always remain within the standard deviation bounds, even if the pictures refer to a given time instant and not to a time average. In the case of temperature fluctuations, the standard bounds are exceeded for $\mathrm{Ma} = 31$, $\mathrm{Kn} = 0.2$ (Fig. 16), but we remark that these bounds are calculated under the assumption that the standard error in the square of the molecular velocity ξ_1 is equal to $\sqrt{2}\, T_x$, which is strictly true only if the underlying distribution is well represented by a Maxwellian. On the contrary, the results of Section 7 show that, with the increase of $\mathscr{T}$, this hypothesis no longer holds.

6. RESULTS OF THE TWO-DIMENSIONAL SIMULATION

We performed the two-dimensional calculations with the same values of Mach and Knudsen numbers as before in a square domain 10×50 cells wide with 2000 particles per cell, to verify that homogeneity was maintained. The results agree completely with the one-dimensional ones both in the time evolution of moments (whose graphs are not shown, being a copy of those discussed in the previous section) and with respect to the space homogeneity which maintains itself in the statistical bounds proper to the reduced size of the sample, as can be seen from Figs. 17 and 18 relative to the profiles of the x component of the velocity taken at the same instant at two different values of x.

7. THE DISTRIBUTION FUNCTION

In the one-dimensional case we also computed the distribution function normalized as a probability in velocity space and compared it with an

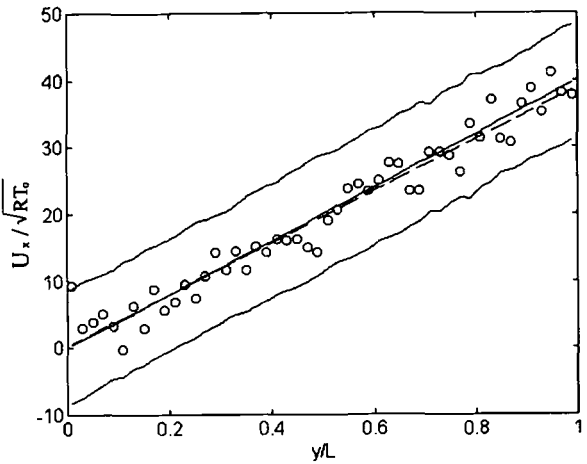

Fig. 17. Tangential velocity profile at $2.4\mu/p$ and $x = L/2$; $\mathrm{Kn} = 0.2$, $\mathrm{Ma} = 31$: (○) two-dimensional DSMC with 10×50 cells and 2000 particles per cell, (--) linear fit, (—) theoretical velocity profile ± 3 standard deviations obtained through the calculated temperature T_x.

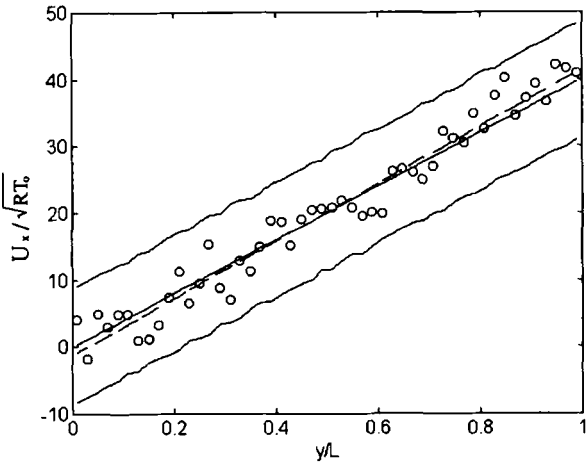

Fig. 18. Tangential velocity profile at $2.4\mu/p$ and $x = 0.5L$; $\mathrm{Kn} = 0.2$, $\mathrm{Ma} = 31$: (○) two-dimensional DSMC with 10×50 cells and 2000 particles per cell, (--) linear fit, (—) theoretical velocity profile ± 3 standard deviations obtained through the calculated temperature T_x.

anisotropic normal distribution f_N. The latter, when referred to suitable axes, can be written as

$$f_N = \frac{1}{2\pi(T_1 T_2)^{1/2}} \exp\left[-\frac{(\xi_1')^2}{2T_1} - \frac{(\xi_2')^2}{2T_2} \right] \tag{7.1}$$

where ξ_1' and ξ_2' are the molecular velocity components with respect to a Cartesian coordinate system rotated by an angle θ with respect to (x, y). Thus

$$\xi_1' = \xi_1 \cos\theta - \xi_2 \sin\theta, \qquad \xi_2' = \xi_1 \sin\theta + \xi_2 \cos\theta \tag{7.2}$$

Equation (7.1) is a good representation for the part of the distribytion close to the bulk velocity, but the tails of the distribution are more populated in the actual distribution than in (7.1). The level surfaces in Figs. 19–21 refer to the values 0.001, 0.01, 0.1, 0.3, 0.5, and 0.8 in terms of the maximum value. Figure 20, which refers to the same case as Fig. 19 but at a later time, shows that, as time passes, the less populated levels differ more and more widely in the approximate analytical representation (7.1) and in the results of the calculations. The angle $\theta = 1.080$ computed by best-fitting is in good agreement with the value 1.097 for the ellipse of the stresses. Figure 21 refers to the higher Mach number Ma = 31. Here the angle varies

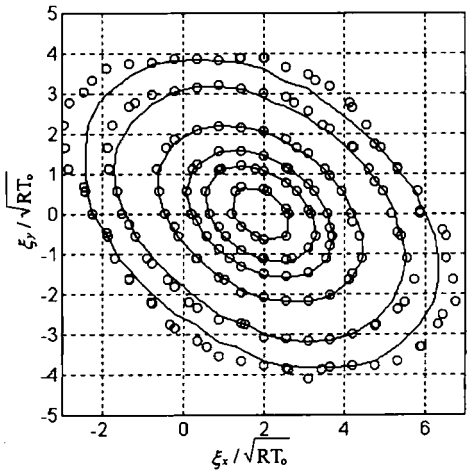

Fig. 19. Isolines of the marginal distribution function integrated along the z direction at $y = L/2$ and time $1.4\mu/p$; Kn = 0.2, Ma = 3: (○) one-dimensional DSMC, (—) fitting by a bivariate normal distribution. Contour lines cut at the fractions 0.001, 0.01, 0.1, 0.3, 0.5, and 0.8 of the DSMC maximum.

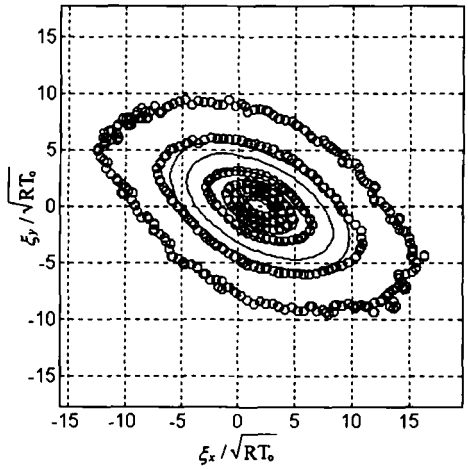

Fig. 20. Isolines of the marginal distribution function integrated along the z direction at $y = L/2$ and time $8.8\mu/p$; Kn = 0.2, Ma = 3: (○) one-dimensional DSMC, (—) fitting by a bivariate normal distribution. Contour lines cut at the fractions 0.001, 0.01, 0.1, 0.3, 0.5, and 0.8 of the DSMC maximum; note that the DSMC line at 0.01 overlaps with the line of the model at 0.001.

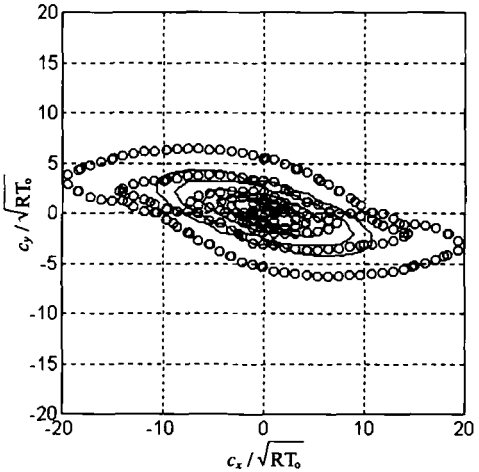

Fig. 21. Isolines of the marginal distribution function integrated along the z direction at time $0.7\mu/p$; Kn = 0.2, Ma = 31: thanks to the homogeneity, it has been referred to the thermal velocities and averaged on the whole field. (○) One-dimensional DSMC, (—) fitting by a bivariate normal distribution. Contour lines cut at the fractions 0.001, 0.01, 0.1, 0.3, 0.5, and 0.8 of the DSMC maximum.

from 1.32 to 1.42 in a time interval of the order $3.5\mu/p$ as compared to the value 1.36 of the ellipse of the stresses.

The fact that the distributions are always symmetrical with respect to their centers ensures that the centered third-order moments, and hence the heat flow, vanish at all times, as predicted by the analytical solution.

The velocity distribution in the (y, z) plane remains perfectly isotropic, ensuring the equality of p_{yy} and p_{zz}, in agreement with the closed-form solution.

8. CONCLUDING REMARKS

We have discussed the results arising from a numerical simulation of the behavior of a monatomic rarefied gas in plane Couette flow with "bounceback" boundary conditions. This behavior agrees with a closed-form solution. From the figures one can also see that most of the computed data lie within the bounds established by standard deviation.

We feel that the validation presented here guarantees that Monte Carlo simulation provides results in good agreement with the Boltzmann equation. This is important not only for applications to high-altitude flight,[1] but also because because this type of simulation has proved to be a good tool for investigating the development of instabilities[16–18] and possibly the transition of a rarefied gas to turbulence.[19]

ACKNOWLEDGMENTS

This research was carried out in the framework of activity of the Gruppo Nazionale di Fisica Matematica of the Italian Research Council (C.N.R.) and was also supported by the Ministero per l'Università e la Ricerca Scientifica e Tecnologica.

REFERENCES

1. G. Bird, Perception of numerical methods in rarefied gasdynamics, in *Rarefied Gas Dynamics: Theoretical and Computational Techniques*, E. P. Muntz, D. P. Weaver, and D. H. Campbell, eds. (AIAA, Washington, D. C., 1989), pp. 212–226.
2. C. Cercignani, *The Boltzmann Equation and Its Applications* (Springer, New York, 1988).
3. C. Cercignani, *Mathematical Methods in Kinetic Theory* (Plenum Press, New York, 1990).
4. C. Cercignani, Exact solutions of the Boltzmann equation, in *Modern Group Analysis: Advanced Analytical and Computational Methods in Mathematical Physics*, N. H. Ibragimov *et al.*, eds. (Kluwer, Dordrecht, 1993), pp. 125–126.
5. C. Cercignani, Kinetic theory with "bounce-back" boundary conditions, *Transport Theory Stat. Phys.* **18**:125 (1989).
6. E. Ikenberry and C. Truesdell, On the pressures and the flux of energy in a gas according to Maxwell's kinetic theory, *I, J. Rat. Mech. Anal.* **5**:1–54 (1956).

7. C. Truesdell and R. G. Muncaster, *Fundamentals of Maxwell's Kinetic Theory of a Simple Monatomic Gas* (Academic Press, New York, 1980).
8. A. A. Nikol'skii, The three-dimensional expansion–contraction of rarefied gas with power interaction functions, *Sov. Phys.-Doklady* **8**:639–641 (1964).
9. R. G. Muncaster, On generating exact solutions of the Maxwell–Boltzmann equation, *Arch. Rat. Mech. Anal.* **70**:79–90 (1979).
10. V. S. Galkin, Exact solutions of the kinetic moment equations of a mixture of monatomic gases, *Fluid Dynamics* **1**:29–34 (1966).
11. C. Cercignani, Existence of homoenergetic affine flows for the Boltzmann equation, *Arch. Rat. Mech. Anal.* **105**:377–387 (1989).
12. V. S. Galkin, On a solution of the kinetic equation, *Prikladnaya Matematika i Mekhanika* **20**:445–446 (1956) [in Russian].
13. V. S. Galkin, On a class of solutions of Grad's moment equations, *Prikladnaya Matematika i Mekhanika* (1958) [in Russian].
14. V. S. Galkin, One-dimensional unsteady solutions of the equations for the kinetic moments of a monatomic gas, *Prikladnaya Matematika i Mekhanika* [in Russian].
15. C. Truesdell, On the pressures and the flux of energy in a gas according to Maxwell's kinetic theory, II, *J. Rat. Mech. Anal.* **5**:55–128 (1956).
16. S. Stefanov and C. Cercignani, Monte Carlo simulation of Bénard's instability in a rarefied gas, *Eur. J. Mech. B* **451**:543–553 (1992).
17. C. Cercignani and S. Stefanov, Bénard's instability in kinetic theory, *Transport Theory Stat. Phys.* **21**:371–381 (1992).
18. S. Stefanov and C. Cercignani, Monte Carlo Simulation of the Taylor–Couette flow of a rarefied gas, *J. Fluid Mech.* **256**:199–213 (1993).
19. S. Stefanov and C. Cercignani, Monte Carlo simulation of channel flow of a rarefied gas, *Eur. J. Mech. B* **12**, to appear (1993).